JOURNAL OF CATALYSIS 130, 86–105 (1991)

Reactions of Neopentane, Methylcyclohexane, and 3,3-Dimethylpentane on Tungsten Carbides: The Effect of Surface Oxygen on Reaction Pathways

FABIO H. RIBEIRO,* RALPH A. DALLA BETTA,* MICHEL BOUDART,*
JOSEPH BAUMGARTNER,† AND ENRIQUE IGLESIA†,[1]

Department of Chemical Engineering, Stanford University, Stanford California 94305; and Corporate Research Laboratories, Exxon Research and Engineering Co., Route 22 East, Annandale, New Jersey 08801

Received November 6, 1990; revised January 31, 1991

High surface area tungsten carbides with WC and β-W_2C structure were prepared by direct carburization of WO_3 in CH_4–H_2 mixtures. Their surfaces appear devoid of excess polymeric carbon and adsorb between 0.2 and 0.4 monolayers of CO and H. These materials are very active in neopentane hydrogenolysis. Chemisorbed oxygen inhibits hydrogenolysis reactions and leads to the appearance of isopentane among the reaction products. Neopentane isomerization to isopentane occurs only on Pt, Ir, and Au surfaces. Thus, oxygen-exposed tungsten carbides catalyze reactions characteristic of noble metal catalysts. 3,3-Dimethylpentane isomerizes much faster than neopentane on oxygen-exposed carbides; the isomer distribution suggests that isomerization proceeds via a methyl shift mechanism rather than through the C_5-ring hydrogenolysis pathways characteristic of highly dispersed Pt. The apparent involvement of 3,3-dimethyl-1-pentene reactive intermediates is consistent with carbenium-type methyl shift pathways. Secondary carbon atoms, capable of forming stable carbenium ions, are present in 3,3-dimethylpentane but not in neopentane; they account for the high 3,3-dimethylpentane isomerization rate and selectivity on oxygen-exposed tungsten carbide powders. Both dehydrogenation and isomerization reactions of methylcyclohexane occur on these carbide powders. These results suggest the presence of a bifunctional surface that catalyzes dehydrogenation and carbenium ion reactions typically occurring on reforming catalysts.

1. INTRODUCTION

The catalytic properties of transition metal carbides have been recently reviewed (*1–3*). Early catalytic studies on tungsten (*4*) and molybdenum (*5*) carbides used materials with low specific surface and possibly containing trace surface concentrations of excess carbon and residual oxygen. Tungsten carbides (5 m^2 g^{-1}) were reported to isomerize neopentane to isopentane (*4*), a rearrangement reaction previously detected only on Pt, Ir, and Au among Group VIII-Ib metals (*7*).

In the present study, we explore this unique property of tungsten carbides using unsupported powders with higher surface areas (30–100 m^2 g^{-1}), stoichiometric surfaces corresponding to WC and β-W_2C, and free of excess polymeric carbon and residual oxygen. Recently, the preparation of high surface area β-W_2C (*8*) and pretreatment methods that remove excess polymeric carbon from molybdenum carbides (*9*) were reported. Here, we report a new procedure for the preparation of high surface area stoichiometric WC and extend surface cleaning procedures to tungsten carbide materials. We also report a unique effect of surface oxygen on the catalytic properties of tungsten carbides; chemisorbed oxygen inhibits neopentane hydrogenolysis while increasing the selectivity to isomerization (isopentane) products.

We also describe the reaction pathways of 3,3-dimethylpentane, a molecular probe

[1] To whom correspondence should be addressed.

0021-9517/91 $3.00

of isomerization mechanisms, on oxygen-exposed WC. These studies suggest that alkane isomerization proceeds by a methyl shift mechanism that involves alkene reactive intermediates. Finally, we report that dehydrogenation and isomerization reactions of methylcyclohexane occur on oxygen-exposed WC, suggesting the presence of a bifunctional surface.

2. EXPERIMENTAL METHODS

2.1 Preparation of High Surface Area WC and β-W_2C Powders

Two tungsten carbide phases (WC and β-W_2C) were used in this study. They were prepared using WO_3 (99.9994%, Johnson-Mathey Puratronic Grade) as the starting material in a flow apparatus previously described (*8*). Typical synthesis experiments required 0.1–0.3 g of starting oxide. A summary of the preparation procedures is included in Scheme 1.

β-W_2C samples were prepared using a previously described procedure (*8*). WO_3 was converted to β-W_2N by exposing it to NH_3 (60 μmol s^{-1}) at 700 K and increasing the temperature from 700 to 1000 K at 8.3×10^{-3} Ks^{-1}. β-W_2C was prepared by carburizing β-W_2N with an 80% CH_4 (Matheson)/20% H_2 (Pd-diffused) mixture (100 μmol s^{-1}) as the sample was heated from 700 to 1150 K at 8.3×10^{-3} K s^{-1}. Polymeric carbon was removed by hydrogen treatment at 973 K for 0.8 h.

A simpler procedure was used to prepare the WC sample. WO_3 was heated in He to 1100 K and then exposed to an 80% CH_4/20% H_2 mixture (100 μmol s^{-1}) at 1100 K for 6 h. Polymeric carbon was removed by a hydrogen treatment at 973 K for 0.8 h.

The effect of chemisorbed oxygen on catalytic and chemisorptive properties was examined by exposing fresh carbide samples to O_2 at RT or 800 K and then treating in flowing H_2 at 673 K for 1 h. Fresh tungsten carbides were exposed to oxygen by leaking O_2 (~0.1 μmol $s^{-1}g^{-1}$) slowly into the preparation cell in order to prevent exotherms and bulk conversion to WO_3. The oxygen uptake by fresh carbide samples at RT was about one monolayer. High uptakes (four to five monolayers) were obtained by subsequently heating these samples to 573–800 K in 20 kPa O_2 for about 0.25 h. Oxygen-exposed samples are identified as WC/O–T_i, where T_i is the exposure temperature. The surface density of chemisorbed oxygen was then reduced to submonolayer levels by a hydrogen treatment at 673 K for 1 h; the oxygen coverage that remains after this treatment increases with increasing oxygen exposure temperature.

Supported Pt and Ru catalysts were used in catalytic comparisons with tungsten car-

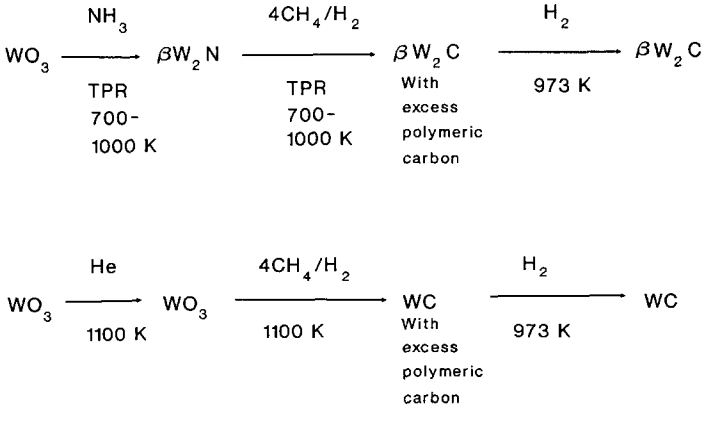

SCHEME 1. Preparation of tungsten carbides.

bides. The 0.5% wt Ru/Al_2O_3 catalyst (Baker) was reduced in flowing H_2 at 673 K for 2 h before catalytic and chemisorption measurements. Ru dispersion, measured by irreversible CO chemisorption, was near 100% (*6, 11*). The 5% Pt/Al_2O_3 catalyst was prepared by incipient wetness impregnation of γ-Al_2O_3 with H_2PtCl_6 (*12*). It was dried, treated in O_2 at 573 K for 30 s, and reduced in H_2 at 673 K for 2 h. Pt dispersion, measured by H_2 titration of surface oxygen, was 75%.

2.2 Surface and Bulk Characterization

The bulk structure of the carbide materials was determined by X-ray diffraction and corresponds to WC and β-W_2C (*13*).

H_2 (Pd-diffused), O_2, and CO (Matheson, ultrahigh purity) chemisorption uptakes were measured at room temperature (RT) in a constant-volume apparatus. Adsorption isotherms were measured between 5 and 20 kPa; backsorption isotherms were obtained by evacuating samples at RT for 0.25 h after adsorption measurements and determining the gas uptake between 5 and 20 kPa. Both adsorption and backsorption isotherms were extrapolated to zero pressure in order to determine the surface density of total and weakly adsorbed species, respectively. The density of irreversible or strongly adsorbed species was obtained by subtracting the extrapolated values of the two isotherms. Specific surface areas (S_g) were measured by dinitrogen (Matheson, Prepurified) physisorption at liquid nitrogen temperatures using the BET method (*14*).

These materials were also characterized by temperature-programmed reduction (TPR) in a mixture of 33% H_2 (Linde, Prepurified) in He (Linde, High Purity) at a total flow rate of 20 μmol s^{-1}. The gas mixture was purified using a liquid nitrogen-cooled molecular sieve trap and a MnO/SiO_2 oxygen getter at RT in order to remove trace O_2 and H_2O impurities. Carbide samples (~0.1 g) were heated from RT to 1370 K at 0.24 K s^{-1} during TPR. Reaction products were analyzed by mass spectrometry (Hewlett–Packard 5970 mass selective detector, scanning mode). Detection limits were 1 ppm for CO and N_2 and 6 ppm for CH_4 and H_2O. This procedure allowed accurate measurements of the carbon and oxygen content in carbide samples.

Temperature-programmed desorption of NH_3 preadsorbed at RT was carried out in pure He (200 μmol s^{-1} g^{-1}) at 0.24 K s^{-1} in the flow apparatus used for TPR experiments.

2.3 Reaction Rates and Selectivity Measurements

Neopentane (Phillips, Research Grade, 99.8%) reaction rates were measured in a gradientless recycle batch reactor (1900 cm^3) at 490 K on fresh carbide catalysts and at 580 and 636 K on O_2-exposed catalysts; neopentane and dihydrogen pressures were 9.8 and 91 kPa, respectively. Reaction products were analyzed by gas chromatography (Hewlett–Packard, FID detection, 30% DC200 on 60/80 Chromosorb P-AW packed column). The analysis protocol permits hydrocarbon concentration measurements as low as 3 ppm in reaction products (3×10^{-6} mol/mol neopentane).

3,3-Dimethylpentane (Wiley, 99.8%) and methylcyclohexane (Fluka, 99.6%) reactions were also studied in a gradientless recirculating reactor (400 cm^3 total volume) at 623 K, and 4.4 kPa hydrocarbon, and 96 kPa dihydrogen pressures on an oxygen-exposed catalyst (WC/O–800 K). Products were analyzed by capillary chromatography using flame ionization and mass spectrometric detection (Hewlett–Packard 5880 GC, 5993A GC/MS).

Reactant conversion is reported as turnovers, defined as the number of reactant molecules converted per surface site in the catalyst charge. Site densities are determined by chemisorption measurements, as previously described. The slope of reactant turnover-time plots is used to calculate turn-

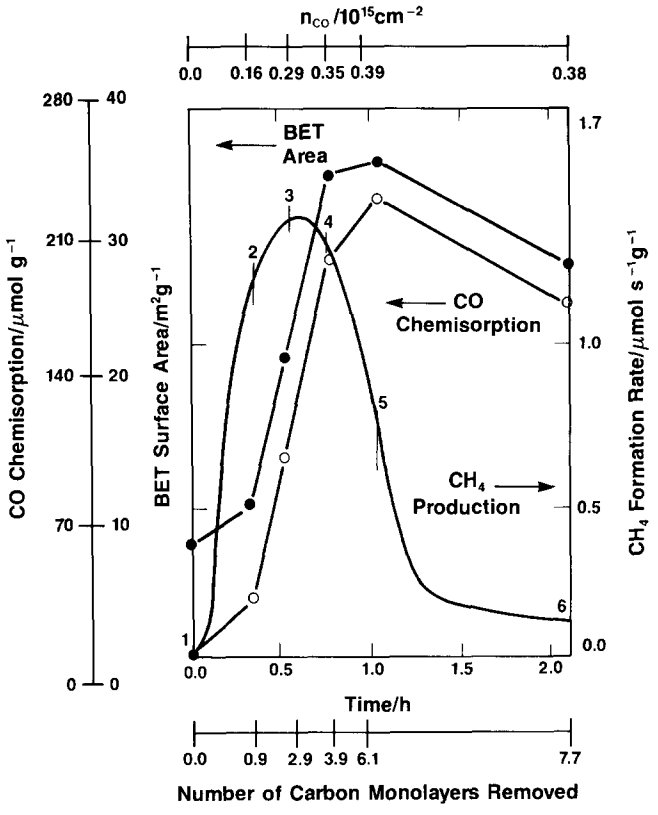

FIG. 1. Carbon removal from WC during H_2 treatment at 973 K. Effect on CO chemisorption uptake and specific surface area.

over rates. Product concentrations are reported as site yields, defined as the number of product molecules present within the reactor per surface site at a given contact time. Site-time yields are obtained from the slope of site yield–time plots; their use instead of turnover rates in reporting product formation rates reflects the difficulty in distinguishing primary and secondary reaction steps that contribute to the multiple products of hydrocarbon reactions. Turnover rates reflect single surface sojourn events, whereas site-time yields simply reflect the integrated effects of primary and secondary reaction events on the observed rate of appearance of individual reaction products. Selectivities are reported as either molar selectivities or as the percentage of converted reactant molecules that appear as a given product (carbon selectivity).

3. RESULTS/DISCUSSION

3.1 Surface Composition

Tungsten carbide powders prepared by direct carburization of WO_3 or β-W_2N precursors did not chemisorb CO or hydrogen at RT; the lack of irreversible chemisorption and their low BET surfaces areas (Fig. 1) suggest extensive contamination by polymeric carbon. The carbon contaminant was removed as methane during a hydrogen treatment at 973 K for 0.5 h. Carbon removal

TABLE 1

Physisorption/Chemisorption Data on Fresh WC and β-W_2C Powders

	β-W_2C	WC
N_2 BET surface area/m^2g^{-1}	100	30
Number density for irreversible RT chemisorption/10^{15} cm^{-2} [a]		
CO	0.24	0.39
H	0.21	0.37
N[b]	0.22	0.34
O	1.03	1.39

[a] 10^{15} $cm^{-2} \simeq$ one monolayer.

[b] From N_2 desorption during temperature-programmed desorption of NH_3.

leads to an increase in irreversible CO chemisorption and BET surface area (Fig. 1). After point 4 in Fig. 1, the surface number density for CO (n_{CO}) remains constant and traces of a W metal phase begin to appear along with WC in the X-ray diffraction pattern. We conclude that no polymeric carbon remains on the surface after a 1-h treatment in H_2 at 973 K; the equivalent of six carbon monolayers are removed as CH_4 during this treatment. These pretreated powders (fresh carbides) were used in catalytic and chemisorption experiments without exposure to air or further pretreatment.

Physisorption and chemisorption results on fresh WC and β-W_2C samples are reported in Table 1. CO, N, and H surface densities are very similar on a given sample, suggesting that strongly adsorbed forms of all these titrants effectively measure tungsten carbide surface sites. On both catalysts, CO, N, and H coverages are below one monolayer. Benziger *et. al.* (*15*) report that a tungsten carbide overlayer W(100)-(5 × 1)C irreversibly adsorbs one monolayer of CO at RT. Our lower uptakes (~0.4 × 10^{15} cm^{-2}) on polycrystalline WC suggest that our carbide powders contain surface planes that do not chemisorb CO irreversibly at RT. For example, Stephan (*16*) reports that WC(0001) single crystals do not chemisorb CO at RT. Single crystals of WC(0001) (*16*) and W(100)-(5 × 1)C (*17*) chemisorb oxygen strongly at RT; it is only removed (as CO) above 1400 K. Thus, oxygen, in contrast with H, CO, and N, titrates tungsten carbide surfaces irrespective of their structure. Indeed, our polycrystalline tungsten carbide powders chemisorb about one monolayer of oxygen at RT (1.03-1.39 × 10^{15} cm^{-2}).

Residual oxygen in fresh carbide powders was detected by the evolution of CO at about 1250 K during TPR. The amount of CO desorbed corresponds to 0.12 and 0.07 oxygen monolayers on WC and β-W_2C, respectively, if all the removed oxygen resides on the surface of the materials.

The presence of carbon-deficient surface sites was ruled out by measuring the reactivity of surface oxygen adatoms with dihydrogen at RT on fresh samples that were recarburized by heat treatment (He, 1000–1100 K) or by reaction with CH_4/H_2 mixtures (1–20% CH_4, 1000 K). Both treatments would replenish any carbon-deficient surface sites and thus increase the fraction of the surface oxygen that can be removed by H_2 at RT; this latter reaction proceeds readily on tungsten carbides but does not occur on tungsten metal surfaces (*18*). In our materials, these pretreatments did not affect the fraction of the chemisorbed oxygen (0.1) that reacts with H_2 at RT on WC and β-W_2C. Thus, we conclude that fresh carbide powders have stoichiometric surfaces that lack W metal sites.

Specific surface areas, irreversible CO uptakes, and residual oxygen surface densities were also measured on fresh carbide samples after O_2 exposure at RT or 800 K and a subsequent H_2 treatment at 673 K (Table 2). Surface areas are unchanged by this treatment but irreversible CO uptakes decrease significantly, suggesting that some chemisorbed oxygen remains after the H_2 treatment. CO uptakes decrease further as the oxygen exposure temperature increases.

The residual oxygen surface density was

TABLE 2

Surface Areas, Chemisorption Uptakes, and Oxygen Content on WC and β-W_2C Powders Exposed to Oxygen

	β-W_2C/O–RT	WC/O–RT[b]	WC/O–800 K[b]
N_2 BET Surface area (m^2g^{-1})	100	30	30.7
Irreversibly chemisorbed CO surface density 10^{15} cm^{-2}[a]	0.081	0.11	0.037
Residual oxygen after H_2 treatment at 673 K/10^{15} cm^{-2}	0.42	0.61	—
Oxygen removed as CO above 973 K during H_2 TPR/10^{15} cm^{-2}	0.52	0.65	—

[a] 10^{15} cm^{-2} ~ one monolayer.
[b] WC/O–RT denote fresh carbide samples exposed to O_2 at temperature T.

measured from the evolution of CO and H_2O during TPR up to 1400 K on oxygen-exposed samples (Fig. 2). On both carbide materials, about 50% of the chemisorbed oxygen is removed by H_2 (as H_2O) below 800 K, while the rest desorbs predominantly as CO above 900 K. Similar TPR experiment after reduction of O-exposed samples in H_2 at 673 K for 2 h, show that the residual oxygen surface densities were 0.42×10^{15} cm^{-2} on β-W_2C and 0.61×10^{15} cm^{-2} on WC (Table 2).

The surface characterization results reported in this section suggest that fresh materials are stoichiometric carbides devoid of excess polymeric carbon and of significant residual surface oxygen. Irreversible oxygen chemisorption on these materials at RT or 800 K and reduction at 673 K results in significant residual surface oxygen (~0.5 monolayer). The catalytic properties of fresh and oxygen-exposed tungsten carbides are described in the sections that follow.

3.2 Neopentane Reactions on Fresh WC and β-W_2C Tungsten Carbides

Fresh tungsten carbides catalyze neopentane hydrogenolysis at 490 K (Table 3, Fig. 3). The reaction products are methane, ethane, propane, and isobutane. Isopentane, a

TABLE 3

Turnover Rates and Product Site-Time Yields for Neopentane Reactions on Fresh Carbides and on Supported Ru (490 K, 9.8 kPa Neopentane, 95 kPa H_2)

Catalyst	$\nu_1/10^{-4}s^{-1}$[a]	STY/10^{-4} s^{-1}[b]					E/kJ mol^{-1}
		C_1	C_2	C_3	iC_4	iC_5	
β-W_2C	10	10	0.9	2.5	6.5	0	120 ± 15
WC	300	600	70	90	100	0	—
0.5% Ru/Al_2O_3	85	150	30	8	40	0	150[b]

[a] Turnover rates (ν_1) and initial site-time yields (STY) based on site densities measured by irreversible CO chemisorption at RT.
[b] Boudart and Ptak (7).

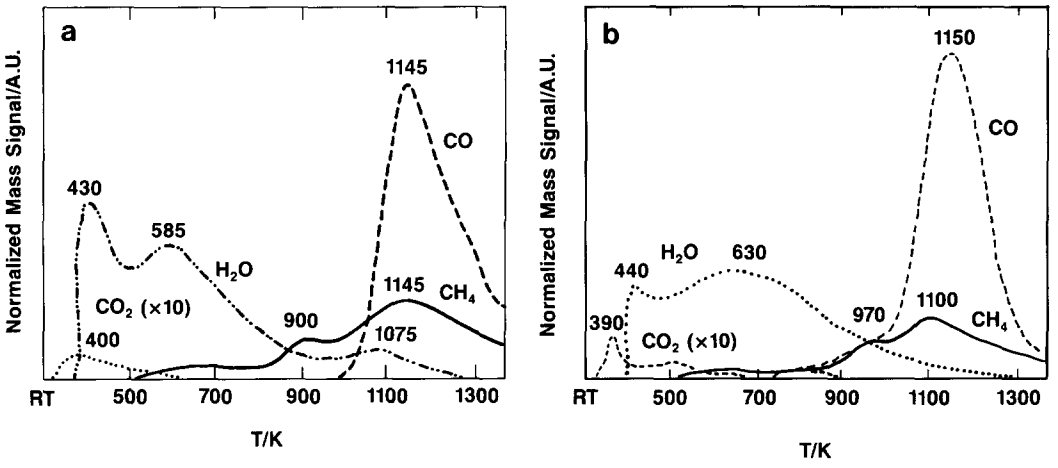

FIG. 2. Temperature-programmed reduction of tungsten carbides after O_2 chemisorption at RT [33% H_2/He]. (a) WC (CO_2, CO, H_2O, and CH_4 amounts were 2, 340, 390, and 205 μmol/g, respectively), (b) β-W_2C (CO_2, CO, H_2O, and CH_4 amounts were 8, 875, 725, and 300 μmol g^{-1}, respectively).

product of neopentane isomerization on Pt and Ir catalysts (*7, 19*), was not detected among the products on fresh WC or β-W_2C catalysts.

The non-zero initial slope of site yield–time plots suggest that all observed hydrocarbons are primary products of neopentane hydrogenolysis on WC and β-W_2C (Figs. 3a and 3b). The initial slopes are used in calculating the individual product site-time yields reported in Table 3. The total neopentane turnover rate is similarly calculated from the data in Fig. 4a and also reported in Table 3. Neopentane hydrogenolysis turnover rates on fresh WC are about 30 times higher than on β-W_2C; they are also significantly higher than on Ru, one of the most active metals for alkane hydrogenolysis reactions (Table 3, Fig. 4a) (*20*). Thus, we conclude that these WC powders are among the most active hydrogenolysis catalysts reported.

The finite initial site-time yields for ethane and propane suggest that several C–C bonds in neopentane are broken in one suface sojourn. The extent of multiple hydrogenolysis can be obtained from the average carbon number ($\bar{n}$) of the product molecules,

$$\bar{n} = \frac{\sum_{i=1}^{4} i\,(\mathrm{STY})_i}{\sum_{i=1}^{4} (\mathrm{STY})_i}, \qquad (1)$$

where i = carbon number, and from the average number of C–C bonds broken per converted neopentane molecule ($\bar{x}$),

$$\bar{x} = \frac{5 - \bar{n}}{\bar{n}}. \qquad (2)$$

The value of $\bar{x}$ increases slightly with contact time on WC and β-W_2C, suggesting a minor contribution of secondary (multiple-surface sojourn) reactions to the observed product distributions (Fig. 4b). The shape of contact time plots for isobutane (Fig. 3) suggests that it is the most reactive primary product, consistent with the hydrocarbon reactivity pattern,

$$i\,C_4 > C_3 > C_2$$

reported by Yao and Shelef (*21*) for neopentane products on Pt catalysts. Values of $\bar{x}$ extrapolated to zero time are 1.9 for WC, 1.1 for β-W_2C, and 1.7–1.9 for Ru/Al_2O_3 catalysts (Fig. 4b). Thus, the probability of multiple-bond cleavage in a single-surface sojourn is significantly higher on WC than

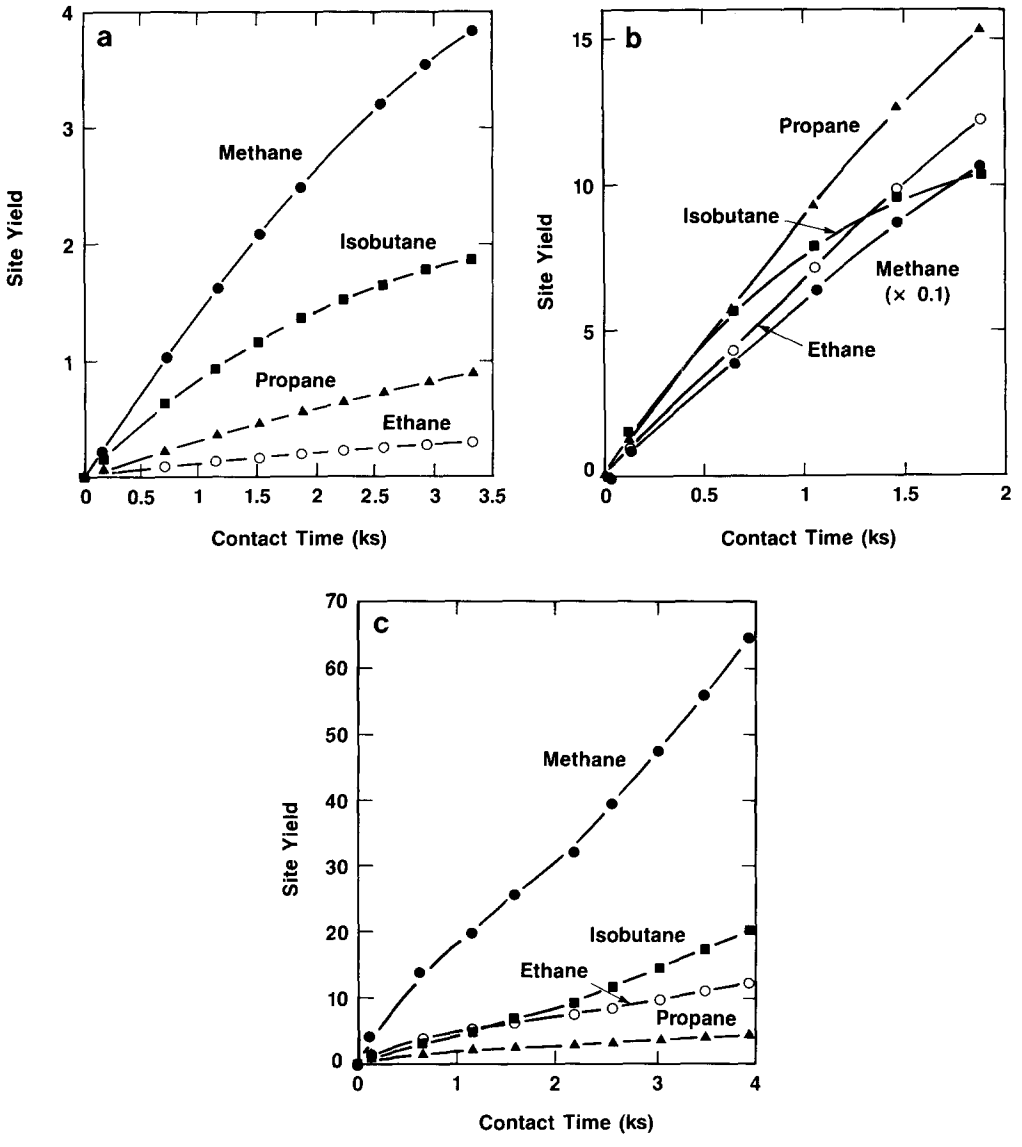

FIG. 3. Neopentane hydrogenolysis site yields on fresh tungsten carbides and Ru catalysts [490 K, 9.8 kPa neopentane, 95 kPa H_2]. (a) β-W_2C (maximum conversion, 0.8%), (b) WC (maximum conversion, 2.6%), (c) 0.5% Ru/Al_2O_3 (maximum conversion, 0.5%).

on β-W_2C, and similar to values obtained on Ru catalysts.

The higher turnover rates and multiple hydrogenolysis probability on WC powders suggest a longer surface lifetime of adsorbed neopentane during a surface sojourn. It appears that neopentane binding energies on WC are considerably higher than those on β-W_2C. The underlying reasons for these differences are unclear at this time; they remain the subject of continuing study.

3.3 Neopentane Reactions on Oxygen-Exposed Tungsten Carbides

O_2 exposure at RT and partial removal of chemisorbed oxygen by H_2 at 673 K decreased neopentane hydrogenolysis rates

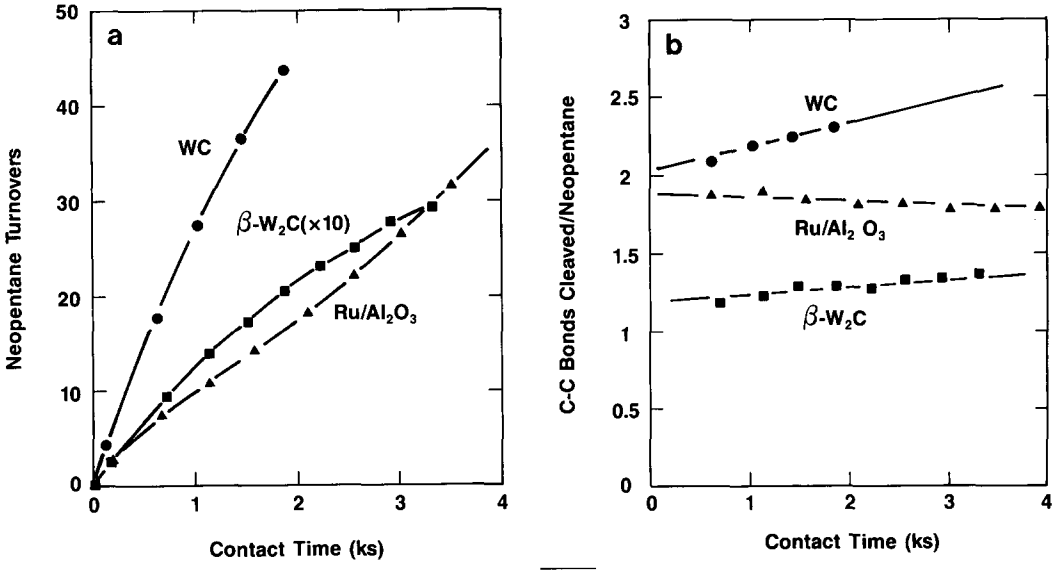

FIG. 4. Neopentane hydrogenolysis turnovers and multiple bond cleavage selectivity on fresh WC and β-W_2C, and on Ru catalysts. (a) total neopentane turnovers, (b) average number of C–C bond cleaved per reacted neopentane [490 K, 9.8 kPa neopentane, 95 kPa H_2].

and multiple-bond cleavage selectivity on WC and β-W_2C; it also led to the appearance of isopentane, an isomerization product, in the reactor effluent (Figs. 5 and 6, Table 4); in addition, traces of *n*-butane, a product of the secondary isomerization of isobutane, were detected among the products. Neopentane reaction products were no longer detectable at 490 K on oxygen-exposed carbide. Therefore, kinetic studies on oxygen-exposed carbides were carried out at 580 K.

Site yield–time plots for all products have non-zero initial slopes, suggesting that they are all primary products of neopentane surface reactions on oxygen-exposed carbides (Fig. 5). Site-time yields, calculated from their initial slopes, are reported in Table 4. Neopentane turnover rates are 10 times higher on WC/O–RT (4.0×10^{-3} s^{-1}) than on β-W_2C/O-RT (3.5×10^{-4} s^{-1}), and similar to those measured on 5% Pt/Al_2O_3 (2.0×10^{-3} s^{-1}) (Fig. 6a, Table 4). However, the isomerization selectivity and isopentane site-time yields on Pt/Al_2O_3 (10^{-3} s^{-1}) are considerably higher than on WC/O–RT (5×10^{-5} s^{-1}) or β-W_2C/O–RT (2×10^{-5} s^{-1}). Also, total neopentane turnover rates on fresh β-W_2C, extrapolated from 490 K using an activation energy of 120 kJ/mol (Table 3), are 300 times greater than their value on β-W_2C/O–RT.

Our results suggest that chemisorbed oxygen (~0.5 monolayer) markedly inhibits neopentane hydrogenolysis on tungsten carbides. Neopentane hydrogenolysis on Pt requires two to three atom ensembles (*22*); if similar structural requirements apply on carbide surfaces, chemisorbed oxygen coverages of 0.5 monolayers should not decrease hydrogenolysis rates by two orders of magnitude. On Pt (*23*) and Ir (*24*), alloying with inactive Au atoms (0–86% at.) did not affect neopentane hydrogenolysis turnover rates, suggesting that active sites consist of single Pt surface atoms.

The inhibiting effect of chemisorbed oxygen on tungsten carbides may reflect their non-uniform surface. Surface sites or ensembles that bind neopentane strongly are

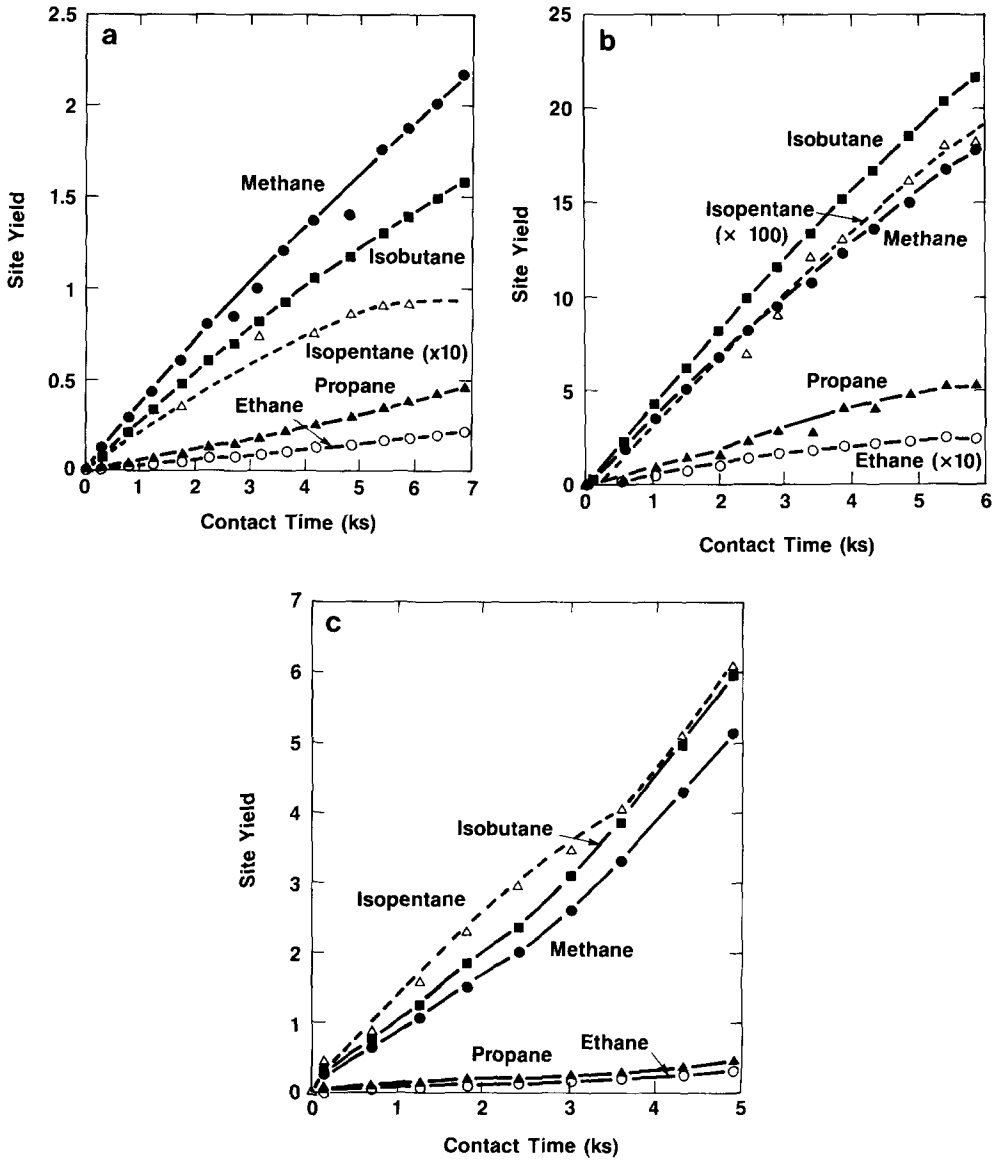

FIG. 5. Neopentane hydrogenolysis and isomerization site yields on oxygen-exposed (RT) tungsten carbides and on Pt catalyst [580 kPa, 9.8 kPa neopentane, 95 kPa H_2]. (a) β-W_2C (maximum conversion, 3.5%), (b) WC (maximum conversion, 3.3%), (c) 5% Pt/Al_2O_3 (maximum conversion, 0.65%).

also likely to chemisorb oxygen with high binding energy. Neopentane hydrogenolysis rates are first order in neopentane pressure and negative order (between -1.0 and -2.0) in dihydrogen pressure (*21, 25, 26*), suggesting that overall rates are limited by either

(i) neopentane chemisorption on hydrogen-covered surfaces or

(ii) bond cleavage of partially dehydrogenated neopentane surface species.

In either case, increasing neopentane binding energy would increase the rate of the limiting step. Thus, it is likely that the

TABLE 4

Turnover Rates and Product Site-Time Yields for Neopentane Reactions on Oxygen-Exposed (at RT) Tungsten Carbides and on Supported Pt (580 K, 9.8 kPa Neopentane, 95 kPa H_2)

Catalyst	$\vartheta_t/10^{-4}$ s^{-1} [a]	STY/10^{-4} s^{-1} [a]				
		C_1	C_2	C_3	iC_4	iC_5
β-W_2C/O–RT	3.5	3.0	0.3	0.6	2.5	0.2
WC/O–RT	40	40	3.0	6.0	45	0.5
5% Pt/Al_2O_3	20	7.5	0.8	0.4	9.0	10

[a] Turnover rates (ϑ_t) and initial site-time yields (STY) based on site densities measured by irreversible CO chemisorption at RT.

chemisorbed oxygen that remains after O_2 exposure at RT and H_2 treatment at 673 K, selectively titrates the most reactive sites for neopentane hydrogenolysis.

Chemisorbed oxygen also decreases the probability of multiple C–C bond cleavage during a surface sojourn. The average number of C–C bonds cleaved per reacted neopentane molecule on WC/O–RT is close to unity, independent of time, and thus unaffected by secondary reactions on all catalysts (Fig. 6b). These data suggest that the binding energy and surface lifetime of adsorbed neopentane reactants decreases markedly, at least on WC, when chemisorbed oxygen is present on the surface (Figs. 4b and 6b).

3.4 Kinetic Analysis of Neopentane Reaction Pathways

Interestingly, chemisorbed oxygen also appears to promote neopentane isomerization on tungsten carbides, possibly by introducing new surface functionalities and reaction paths. Chemisorbed oxygen could also lead to the detection of isopentane among products by merely decreasing the hydrogenolysis rates on the carbide surfaces; this passivating effect would lower the binding energy and surface lifetime of neopentane reactants and of the primary isopentane products and thus would permit isopentane desorption before significant hydrogenolysis occurs. Alternately, chemisorbed oxygen could simply inhibit the hydrogenolysis of desorbed isopentane products during subsequent surface sojourns. In this section, we explore these alternate hypotheses by proposing a neopentane reaction network and using it to examine the relative rates of neopentane and isopentane reactions on tungsten carbides.

The neopentane reaction network described in Scheme 2 is consistent with our previously discussed kinetic data; it accounts for the possible cleavage of several C–C bonds in one surface sojourn and for any secondary reactions of isopentane and isobutane after desorption. It does not include readsorption and sequential hydrogenolysis of ethane and propane because, as discussed previously, they do not contribute significantly to the observed product distribution at the low conversions used in our study.

Isopentane and isobutane are Bodenstein-type reactive gas-phase intermediates (*27*) in neopentane reactions on tungsten carbides; they reach steady-state concentrations given by

$$\frac{(i - C_5)_{ss}}{(\text{neo} - C_5)} = \frac{k_1}{k_2}, \quad k_2 \gg k_1 \qquad (3)$$

and

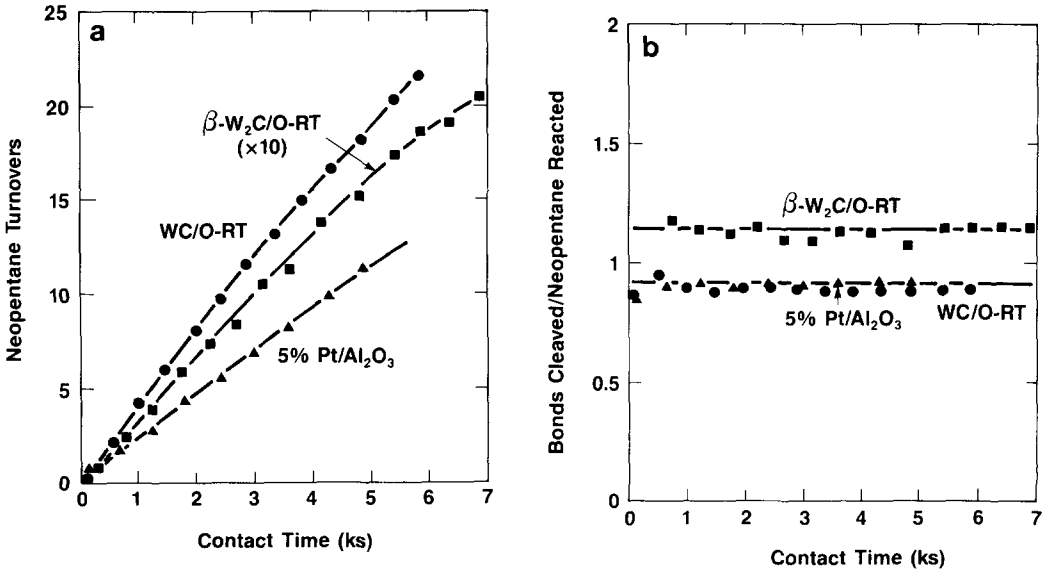

FIG. 6. Neopentane reaction turnovers and multiple bond cleavage selectivity on oxygen-exposed WC and β-W_2C, and on Pt Catalyst. (a) total neopentane turnovers, (b) average number of C–C bonds cleaved per reacted neopentane [580 K, 9.8 kPa neopentane, 95 kPa H_2].

a) Surface Reaction Network

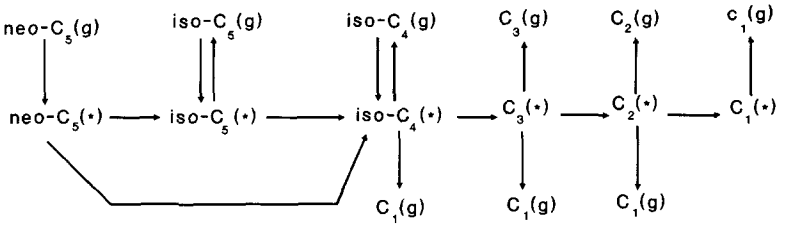

b) Simplified Kinetic Network

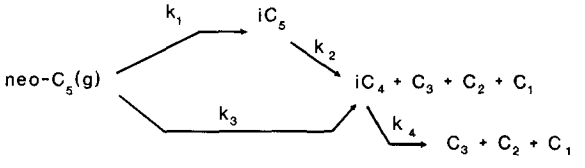

(a) all reaction first order in hydrocarbon [21,25,26]

SCHEME 2. Neopentane reaction network.

TABLE 5

Kinetic Rate Constant Ratios for Neopentane Reactions on β-W_2C and β-W_2C/O–RT (See Scheme 2 for Definitions)

	β-W_2C[a]	β-W_2C/O–RT[c]
k_1/k_2	3×10^{-7} [b]	4×10^{-4}
$\frac{k_1 + k_3}{k_4}$	$\gg 0.01$	$\gg 0.06$
$\frac{k_2}{k_3}$	~ 200	~ 20

[a] 490 K.
[b] Calculated following procedure described in text.
[c] 580 K.

$$\frac{(i - C_4)_{ss}}{(neo - C_5)} = \frac{k_2 x_2}{k_4}\frac{(i - C_5)_{ss}}{(neo - C_5)} + \frac{k_3 x_3}{k_4} = \frac{k_1 x_2 + k_3 x_3}{k_4}, \quad (4)$$

where x_2 and x_3 are the fractional isobutane selectivities in isopentane and neopentane conversion reactions, respectively.

Steady-state isopentane to neopentane concentration ratios were 4.0×10^{-4} on β-W_2C/O–RT (Fig. 5a) and 3.5×10^{-4} on WC/O–RT (Fig. 5b) at 580 K. Isobutane concentrations do not reach their steady-state value at our experimental contact times but continue to increase with reaction time, suggesting that

$$\frac{(i\text{-}C_5)_{ss}}{(neo\text{-}C_5)} = \frac{k_1 + k_3}{k_4} \gg 0.06 \quad (\text{for } \beta\text{-}W_2C/O\text{–RT}), \quad (5)$$

where 0.06 is the value of this ratio at our highest contact time. On fresh β-W_2C at 490 K, this value is much greater than 0.01 (Table 5). Competitive reactions of neopentane and isopentane were used to measure the relative value of their hydrogenolysis rate constants (k_2 and k_3) on fresh β-W_2C (at 490 K) and on β-W_2C/O–RT (at 580 K); their values are reported in Table 5.

In order to estimate the expected isopentane steady-state concentration on fresh β-W_2C at 490 K, we assume that Scheme 2 describes kinetic processes on both oxygen-exposed (k_i) and fresh (k_i') surfaces. From previous discussions, we concluded that

$$k_3' = k_3 \cdot 300$$
$$\frac{k_2'}{k_3'} = 200 \quad (6)$$
$$\frac{k_1}{k_2} = 4 \times 10^{-4}.$$

We also assume here that chemisorbed oxygen affects isomerization only by site blockage and that

$$k_1 = \theta_0 \cdot k_1' = 0.5 \cdot k_1'. \quad (7)$$

Therefore, the concentration of isopentane at steady-state on fresh β-W_2C is obtained by combining the appropriate rate constants in Table 5,

$$\frac{(i\text{-}C_5)_{ss}}{(neo\text{-}C_5)} = \frac{k_1'}{k_2'} = \frac{1}{1500}\cdot\frac{k_1}{k_2} = 3 \times 10^{-7}, \quad (8)$$

a value well below the detection limit ($\sim 3 \times 10^{-6}$) in our experimental setup.

The above analysis was carried out using kinetic rate constants at 580 K, while reactions on fresh samples were carried out at 490 K. However, if the neopentane isomerization and hydrogenolysis activation energies differ by less than 60 kJ mol^{-1}, steady-state isopentane concentrations on fresh samples remain well below the detection limit. This appears to be a reasonable assumption because this activation energy difference is greatest on Pt among Group VIII metals, and it equals 40 kJ mol^{-1} (7).

Clearly, the inhibiting effect of chemisorbed oxygen on hydrogenolysis reactions is sufficient to explain the appearance of isopentane among neopentane reaction products on oxygen-exposed tungsten carbides. We cannot rule out, however, that surface oxygen species also provide or promote surface sites capable of isomerizing neopentane to isopentane. A bond shift mechanism, evolving the direct formation

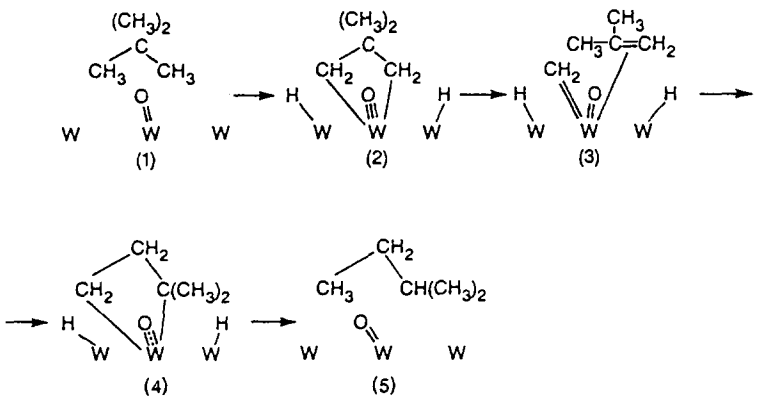

SCHEME 3. Tungstenacyclobutane mechanism for neopentane isomerization (adapted from Refs. (*29, 30*)).

of metallacyclobutanes from neopentane (Scheme 3) has been proposed for neopentane isomerization on Pt (*28, 29*). Chemisorbed oxygen is known to stabilize these metallacycle intermediates that also appear in alkane metathesis reactions (*30*). Tungsten oxides are well-known heterogeneous metathesis catalysts (*31*), and tungstenacyclobutane complexes have been isolated (*32*).

The effect of oxygen in modifying the surface chemistry of model tungsten carbides is well established. The rate and selectivity in ethanol and acetaldehyde decomposition on W(100)-(5 × 1)C depend on the surface carbon-to-oxygen ratio (*33*). On the same surface, chemisorbed oxygen inhibits H_2 and CO chemisorption, and formaldehyde and methanol adsorption and decomposition (*17*). Oxygen lowers the rate of ethylene hydrogenation on tungsten carbides (*34*) and of ethane hydrogenolysis on molybdenum carbides (*35*). In electrocatalytic H_2 oxidation on a WC anode, the active site appears to be oxygen-substituted tungsten carbide (*36*). Also, when H_2 reacts with adsorbed oxygen on WC, the water formed accelerates spillover of hydrogen from WC to oxidized parts of the WC surface, forming H_xWO_3 and enhancing the uptake of H_2 (*37*).

Alkane isomerization also occurs on acid sites but requires, in general, a dehydrogenation functionality in order to convert reactants into reactive olefin intermediates (*38*). Such bifunctional chemistry provides the basis for catalytic reforming processes (*39*). Chemisorbed oxygen leads to the formation of surface WO_x species; supported surface WO_x species are strong acids (*40, 41*), but require the presence of noble metals for alkane isomerization to occur.

Conventional catalytic acid chemistry involves carbenium ions and Lewis and Brønsted sites consisting of polarized surface oxygens or bare metal cations on oxide surfaces (*38*). Carbenium ions are generally formed by protonation of adsorbed olefins with surface H^+ or with other protonated surface hydrocarbons. Isomerization of molecules unable to form olefin intermediates (e.g., neopentane), or those that require primary carbenium ions in reactants or products, apparently require the formation of pentavalent carbon atoms (*42*) or radical cations (*43*). The reaction pathways of such surface species resemble radical chemistry rather than carbonium ion chemistry, with the consequent ability to form and rearrange stable primary radical species (*43*). Such radical-like or monomolecular acid chemistry involves hydride ion or hydrogen radical abstraction from adsorbed paraffins (*44*) and proceeds at considerably lower rates and higher temperatures than conventional ole-

fin-mediated acid chemistry; it leads preferentially to C_2 and C_1 leaving groups rather than to the C_{3+} products typical of acid catalysis (*42*). This accounts for most isomerization products at low temperatures (≤673 K) even for alkanes capable of forming olefin intermediates and stable carbonium ions.

Olah *et al.* (*46*) observed isopentyl cations and H_2 products during neopentane reactions on liquid superacids. More recently, Engelhardt and Hall (*47*) observed isopentane products during neopentane reactions on partially dealuminated Y-zeolites. The isopentane selectivity at 703 K and 10 kPa neopentane was 3.5% and the isopentane site-time yield (per Al atom) was 1.6×10^{-6} s^{-1}. Neopentane reactions were self-poisoning and led to rapid deactivation of the zeolite catalysts.

3.5 3,3-Dimethylpentane Reactions on Oxygen-Exposed Tungsten Carbides (WC/O–800 K)

3,3-Dimethylpentane can isomerize via olefin (3,3-dimethyl-1-pentene) intermediates on acid sites. Acid-catalyzed cracking, however, is slow because of the absence of C_{3+} leaving groups in 3,3-dimethylpentane. Therefore, acid-catalyzed isomerization of 3,3-dimethylpentane proceeds via carbonium ion rearrangements of olefin intermediates,

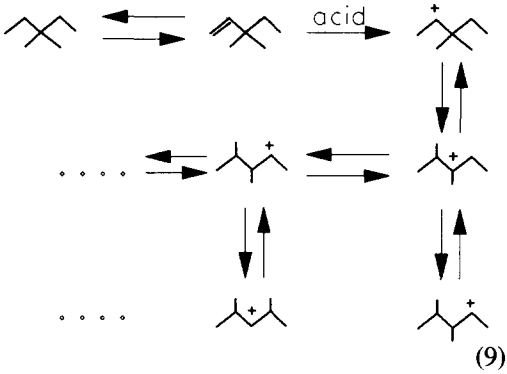

(9)

to give predominantly a mixture of 2,3- and 2,4-dimethylpentanes. Direct cracking, however, is likely to involve radical cation species that favor the cleavage of C_1 and C_2 groups.

3,3-Dimethylpentane is a sensitive molecular probe of isomerization pathways (*10*). The isomer distributions differ among carbonium-ion pathways (reaction (9)), C_5-ring hydrogenolysis processes, typical of highly dispersed Pt (reaction (10)),

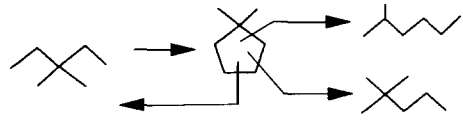

(10)

and metallacyclobutane bond-shift mechanisms (Scheme 3),

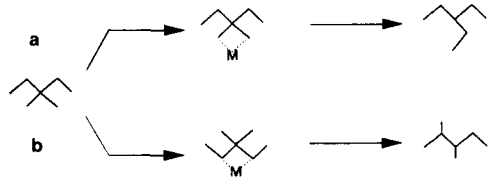

(11a) (11b)

Isomerization rates for neopentane (via Scheme 3) and for 3,3-dimethylpentane via either (11a) or (11b) should be similar. Therefore, we expect that metallacyclobutane intermediates for 3,3-dimethylpentane isomerization on WC/O–800 K would lead to reaction rates similar to those of neopentane.

Turnover rates and cracking and isomerization selectivities for 3,3-dimethylpentane reactions on WC/O–800 K are shown in Fig. 7a. Individual isomer selectivities depend weakly on residence time and extrapolate to non-zero values at zero residence time (Fig. 7b). The predominant reaction product is 2,3-dimethylpentane, the initial product of the carbenium ion methyl shift reactions (reaction 9); 2,3- and 2,4-dimethylpentane approach thermodynamic equilibrium with each other but not with 2,2-dimethylpentane or methylhexane isomers. This behavior is characteristic of carbenium ion rearrangements because chain lengthening to methyl isomers requires primary carbenium ion intermediates,

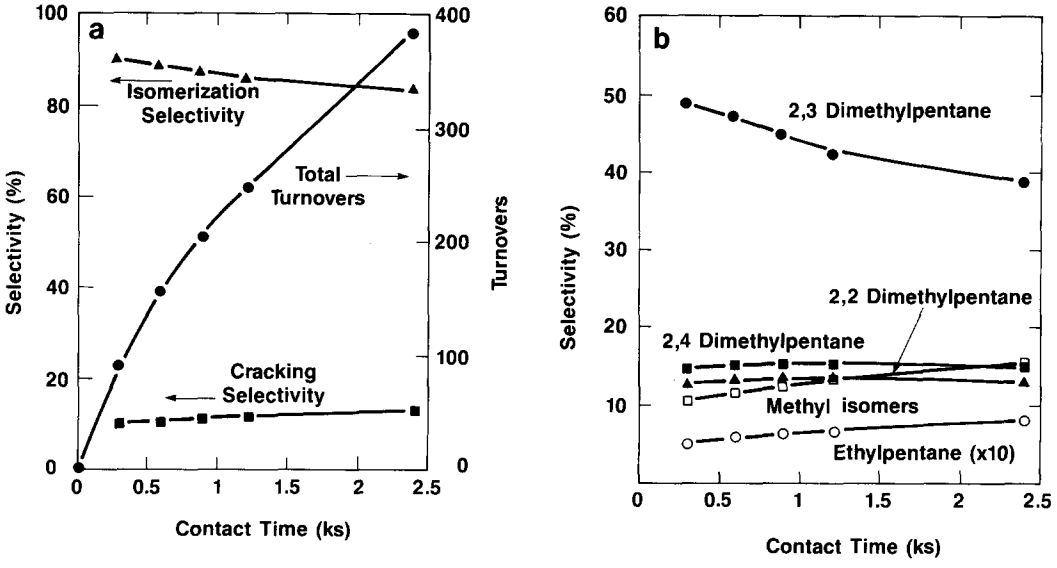

FIG. 7. 3,3-Dimethylpentane Reactions on WC/O–800 K. (a) Turnovers and cracking/isomerization selectivities, (b) isomer selectivities, [623 K, 4.5 kPa, 3,3-dimethylpentane, 96 kPa H_2; maximum conversion 24.8%].

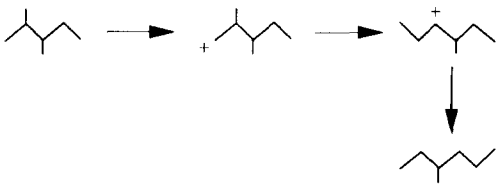

(12)

and because the formation of products with quaternary carbons requires penta-coordinated carbon species in the reaction transition state.

The low initial selectivities to 2,2-dimethylpentane and 2-methylhexane (12% and 4%, Fig. 7b) suggest that C_5-ring hydrogenolysis is not a significant 3,3-dimethylpentane isomerization pathway. Moreover, the trace ethylpentane concentrations (~0.4%) among initial products show that metallacyclobutane intermediates are at most minor 3,3-dimethylpentane isomerization intermediates. However, ethylpentane site-time yields (1.2 s^{-1}) are much higher than neopentane to isopentane site-time yields (~0.04 s^{-1}). Thus, metallacyclobutane intermediates could account for the observed neopentane isomerization rate on oxygen-exposed tungsten carbides, even though they account for only a minor fraction of 3,3-dimethylpentane products.

The primary formation of 2,3- and 2,4-dimethylpentane products (with 52 and 15% selectivity, respectively) and the detection of low but measurable steady-state concentrations of 3,3-dimethyl-1-pentene suggest that 3,3-dimethylpentane isomerization proceeds via acid-catalyzed carbenium ion rearrangements of olefin intermediates; these isomerization pathways are unavailable to neopentane molecules. Related isotopic tracer studies of *n*-alkane isomerization on oxygen-exposed WC support these conclusions. The methylcyclohexane isomerization and NH_3 desorption studies described in the last two sections of this paper also support the presence of acid sites and of acid-catalyzed rearrangements on WC/O–800 K.

Turnover rates and site-time yields for neopentane and 3,3-dimethylpentane are compared in Table 6. Cracking site-time yields are only tenfold higher for 3,3-dimethylpentane than for neopentane, reflecting

TABLE 6

Turnover Rates and Site-Time Yields for Neopentane and 3,3-Dimethylpentane Reactions on Oxygen-Exposed WC

Reactant	3,3-Dimethylpentane[a]	Neopentane[b]
$\mathcal{U}_t/10^{-3}$ s^{-1}	310	3.8
STY/10^{-3} s^{-1}[c]		
C_1–C_{n-1}	35	3.77
Isomerization	275	0.04
S_i(%)[c]		
C_1–C_{n-1}	11.4	99.2
Isomerization	88.6	0.8

[a] 623 K, 4.5 kPa hydrocarbon, 95 kPa H_2, WC/O–800 K.

[b] 580 K, 9.8 kPa hydrocarbon, 95 kPa, H_2, WC/O–RT.

[c] Site-time yields (STY), and selectivities (S_i) are reported on a carbon-basis, using the fraction of the converted reactant molecules appearing as a given product.

the slightly higher temperature (623 K vs 580 K), the larger number of reactive C–C bonds in 3,3-dimethylpentane reactions, and the presence of C_2 leaving groups in 3,3-dimethylpentane but not in neopentane. Isomerization site-time yields are, however, about 10^4 times greater for 3,3-dimethylpentane than for neopentane. The isomerization selectivity (on a carbon basis) is also much higher for 3,3-dimethylpentane (88.6%) than for neopentane (0.8%). These differences are unlikely to arise from a 50 K temperature difference or from merely increasing the number of carbons available for surface attachment. They suggest a distinct shift in the available reaction pathways as secondary carbons and as the ability to form olefins are introduced into the reactant molecule.

We conclude that 3,3-dimethylpentane rearranges via olefin intermediates and conventional carbenium ion chemistry (*38*) on WC/O–800 K but probably cracks to C_1 and C_2 fragments via radical cation intermediates (*43*) because of the absence of stable protonated leaving groups. Neopentane isomerization proceeds via metallacyclobutane species (as on Pt) or pentavalent or radical-like carbenium ion intermediates at rates significantly lower than those of conventional olefin-mediated carbenium ion reaction and with preferential formation of C_1 leaving groups.

3.6 Methylcyclohexane Reactions on Oxygen-Exposed Tungsten Carbides

The bifunctional dehydrogenation–isomerization nature of oxygen-exposed tungsten carbides was also demonstrated by studying the reactions of methylcyclohexane on WC/O–800 K. Methylcyclohexane dehydrogenates to toluene on metal surfaces but isomerizes to ethylcyclopentane and dimethylcyclopentanes only on acidic metal oxides (*38*). Figure 8 shows that both reactions occur readily on WC/O–800 K. The alkylcyclopentane to toluene ratio extrapolates to a value of 0.4 at zero residence time, suggesting a significant contribution of acid-catalyzed pathways to methylcyclohexane reaction products. The decrease in this ratio as conversion proceeds reflects a selective inhibition of acid-catalyzed pathways by the toluene product of the dehydro-

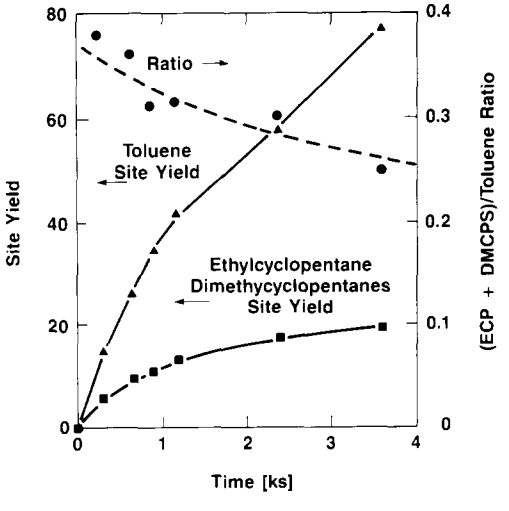

FIG. 8. Methylcyclohexane dehydrogenation (to toluene) and isomerization (to alkylcyclopentanes) on WC/O–800 K [623 K, 4.5 kPa hydrocarbon, 96 kPa H_2; maximum conversion, 25%].

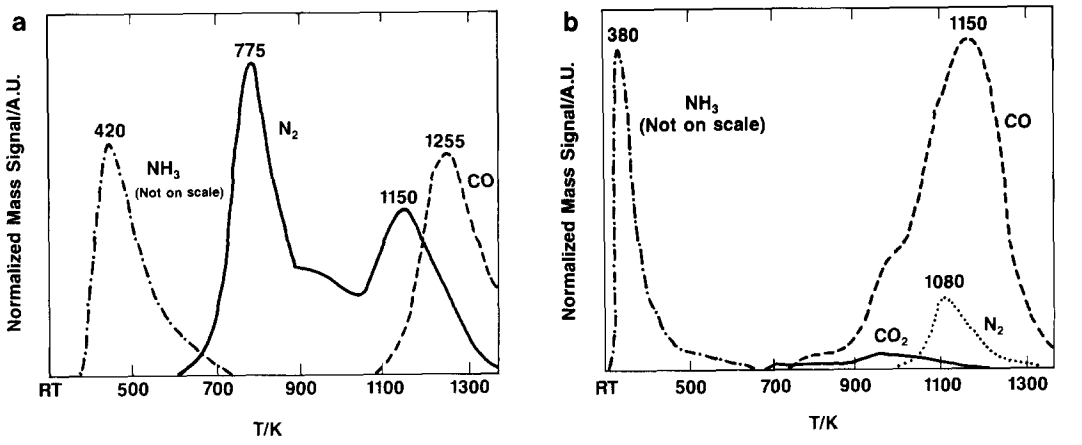

FIG. 9. Temperature-programmed desorption of NH_3 preadsorbed at RT. (a) Fresh β-W_2C (NH_3, N_2, and CO desorbed amounts were 13, 169, and 57 μmol g^{-1}, respectively), (b) β-W_2C/O–RT (NH_3, N_2, and CO desorbed amounts were 90, and 885 μmol g^{-1}, respectively. [He carrier gas; oxygen-exposed sample reduced in H_2/673 K/2 h before NH_3 adsorption at RT].

genation reaction. The effect of contact time on the concentration of methylcyclohexene products suggests that they are reactive intermediates (in equilibrium with reactants) in methylcyclohexane isomerization on WC/O–800 K. Such olefin intermediates are required for cycloalkane isomerization via carbenium ions on acid catalysts.

3.7 Temperature-Programmed Desorption of Preadsorbed Ammonia on Fresh and Oxygen-Exposed Tungsten Carbides

The presence of acid sites on fresh and oxygen-exposed tungsten carbides was tested by measuring the binding energy of molecularly adsorbed NH_3 and its probability of dissociation to adsorbed nitrogen and hydrogen species.

Chemisorbed oxygen leads to a marked increase in the amount of preadsorbed NH_3 that desorbs unreacted during TPD (Figs. 9a and 9b); it also decreases the probability of its surface dissociation to adsorbed N atoms. Thus, oxygen passivates reactive sites capable of irreversible NH_3 adsorption and decomposition near RT. The enhanced desorption of intact NH_3 molecules suggests the presence of acid sites, capable of interacting reversibly with a base (NH_3) near RT, and of subsequently desorbing it without extensive dissociation. The shift in desorption temperature from 420 to 380 K (Fig. 9) suggests that the binding energy of molecularly adsorbed ammonia decreases as chemisorbed oxygen coverage increases. In effect, chemisorbed oxygen appears to passivate strongly interacting (metal-like) sites and to introduce weakly interacting (acid-like) sites on tungsten carbide surfaces.

4. CONCLUSIONS

Fresh tungsten carbides with WC and β-W_2C structures catalyze neopentane hydrogenolysis with turnover rates similar to those on Ru catalysts. Chemisorbed oxygen strongly inhibits neopentane hydrogenolysis and the probability of multiple-bond cleavage during one surface sojourn, suggesting a marked decrease in neopentane binding energy. Chemisorbed oxygen also leads to the appearance of isopentane among reaction products. Neopentane isomerization could involve either metallacyclobutane intermediates on O-modified carbide sites or radical or pentavalent carbenium ions on acidic WO_x surface species.

The presence of acid sites on oxygen-exposed carbides is consistent with the in-

hibited dissociation of preadsorbed NH_3 as oxygen coverage increases. The high isomerization rates and selectivity for molecules containing secondary carbon atoms and capable of forming olefin intermediates by dehydrogenation also supports this conclusion. The isomer distribution from 3,3-dimethylpentane suggests that carbenium ion rearrangements of olefin intermediates account for the predominant isomerization products. Both methylcyclohexane dehydrogenation and isomerization occur on oxygen-exposed WC, suggesting that such materials possess a bifunctional surface capable of catalyzing both dehydrogenation and carbenium ion reactions that typically occur on conventional reforming catalysts.

ACKNOWLEDGMENTS

This work was supported by the Department of Energy Grant DE FG03 87ER13762 and by the Exxon Research and Engineering Co. The use of analytical instruments at Catalytica, at the Center for Materials Research at Stanford and at the Corporate Research Laboratories of Exxon Research and Engineering Co. is gratefully acknowledged. One of us (F.H.R.) thanks CNPq of Brazil for a graduate fellowship.

REFERENCES

1. Levy, R. B., *in* "Advanced Materials in Catalysis" (J. J. Burton and R. L. Garten, Eds.), pp. 101–127. Academic Press, New York, 1977.
2. Oyama, S. T., and Haller, G. L., *in* "Catalysis; Spec. Per. Repts," Vol. 5, pp. 333–365. Roy. Soc. Chem., London, 1982.
3. Leclerq, L., *in* "Surface Properties and Catalysis by Non-Metals" (J. P. Bonnelle, B. Delmon, and E. Derovane, Eds.), p. 433. Reidel, Dordrecht, 1983.
4. Levy, R. B., and Boudart, M., *Science* **181,** 547 (1973).
5. Boudart, M., Oyama, S. T., and Leclerq, L., *in* "Proceedings, 7th International Congress on Catalysis Tokyo, 1980" (T. Seiyama and K. Tanabe, Eds.), pp. 578–590. Elsevier, Amsterdam, 1981.
6. Lee, J. S., Locatelli, S., Oyama, S. T., and Boudard, M., *J. Catal.* **125,** 157 (1990).
7. Boudart, M., and Ptak, L. D., *J. Catal.* **16,** 90 (1970).
8. Volpe, L., and Boudart, M., *J. Solid State Chem.* **59,** 332 (1985).
9. Lee, J. S., Oyama, S. T., and Boudart, M., *J. Catal.* **106,** 125 (1987).
10. Iglesia, E., Baumgartner, J., Price, G. L., Rose, K. D., and Robbins, J. L., *J. Catal.* **125,** 95 (1990).
11. Lee, J. S., Ph.D. thesis, Stanford University, 1984.
12. Rivera-Latas, F., Ph.D. thesis, Stanford University (1986).
13. W. F. McClure, Ed., "Inorganic Compounds," Powder Diffraction File, JCPDS, Swathmore, 1980.
14. Smith, J. M., "Chemical Engineering Kinetics," 3rd ed. McGraw–Hill, New York, 1981.
15. Benziger, J. B., Ko, E. I., and Madix, R. J., *J. Catal.* **54,** 414 (1978).
16. Stephan, P. M., Ph.D. thesis, Stanford University, 1983.
17. Ko, E. I., and Madix, R. J., *J. Phys. Chem.* **85,** 4919 (1981).
18. Boudart, M., Dalla Betta, R. A., Ribeiro, F. H., and Guskey, G. J., submitted for publication.
19. Wong, T. C., Chang, L. C., Haller, G. L., Oliver, J. A., Scarfe, N. R., and Kemball, C., *J. Catal.* **87,** 389 (1984).
20. Sinfelt, J. H., *in* "Advances in Catalysis" (D. D. Eley, H. Pines, and P. B. Weisz, Eds.), Vol. 23, p. 91. Academic Press, New York, 1973.
21. Yao, H. C., and Shelef, M., *J. Catal.* **73,** 76 (1982).
22. Anderson, J. R., and Avery, N. R., *J. Catal.* **5,** 446 (1966).
23. Foger, K., and Anderson, J. R., *J. Catal.* **61,** 140 (1980).
24. Foger, K., and Anderson, J. R., *J. Catal.* **64,** 448 (1980).
25. Yao, H. C., and Shelef, M., *J. Catal.* **56,** 12 (1979).
26. Kikuchi, E., Tsurumi, M., and Morita, Y., *J. Catal.* **22,** 226 (1971).
27. Boudart, M., and Djega-Mariadassou, "Kinetics of Heterogeneous Catalytic Reactions." Princeton Univ. Press, Princeton, NJ, 1984.
28. Garin, F., and Gault, F. G., *J. Am. Chem. Soc.* **97,** 4466 (1975).
29. Parhsall, G. W., Thorn, D. L., and Tulip, T. H., *Chemtech* **12,** 571 (1982).
30. Rappe, A. K., and Goddard, W. A., *J. Am. Chem. Soc.* **104,** 448 (1982).
31. Heckelsberg, L. F., Banks, R. L., and Bailey, G. C., *Ind. Eng. Chem. Prod. Res. Dev.* **7,** 29 (1968).
32. Ephritikhine, E., Green, M. L. H., MacKenzie, R. E., *J. Chem. Soc. Chem. Commun.*, 619 (1976).
33. Ko, E. I., and Madix, R. J., *J. Catal.* **73,** 161 (1982).
34. Kojima, I., Myazaki, E., Inoue, Y., and Yasumori, I., *J. Catal.* **59,** 472 (1979).
35. Ranhotra, G. S., Bell, A. T., and Reimer, J. A., *J. Catal.* **108,** 24 (1987).
36. Ross, P. N., and Stonehart, P., *J. Catal.* **48,** 42 (1977).
37. Boudart, M., Lee, J. S., Imura, K., and Yoshida, S., *J. Catal.* **103,** 30 (1987).
38. Pines, H., "The Chemistry of Catalytic Hydrocar-

bon Conversions." Academic Press, New York, 1981.

39. Sinfelt, J. H., *in* "Catalysis Science and Technology" (J. R. Anderson and M. Boudart, Eds.), Vol. 1, p. 257. Berlin/New York Springer-Verlag, 1981.

40. Ogata, E., Kayima, Y., and Ohta, N., *J. Catal.* **29,** 296 (1979).

41. Soled, S. L., McVicker, G. B., Murrell, L. L., Sherman, L. G., Dispenierre, N. C., Hsu, S. L., and Waldman, D., *J. Catal.* **111,** 286 (1988).

42. Olah, G., *J. Am. Chem. Soc.* **94,** 808 (1972).

43. McVicker, G. B., Kramer, G. M., and Ziemiak, J. S., *J. Catal.* **83,** 286 (1983).

44. Haag, W. O., and Dessau, R. M., *in* "Proceedings, 8th International Congress on Catalysis, Berlin, 1984," Vol. 2, p. 305. Dechema, Frankfurt-am-Main, 1984.

45. Mieville, R. L., and Meyers, B. L., *J. Catal.* **74,** 196 (182).

46. Olah, G. A., Surya Prakash, G. K., and Sommer, J., "Superacids." Wiley, New York, 1985; Olah, G. A., *Angew. Chem. Int. Ed.* **12,** 173 (1973).

47. Engelhardt, and Hall, W. K., *J. Catal.*, **125,** 472 (1990).